IEEE Access
Multidisciplinary | Rapid Review | Open Access Journal

Received June 3, 2019, accepted June 16, 2019, date of publication June 21, 2019, date of current version July 16, 2019.

Digital Object Identifier 10.1109/ACCESS.2019.2924347

Model Classification-and-Selection Assisted Robust Receiver for OFDM Systems

XIAOYING ZHANG[1], KAI MEI[1], (Student Member, IEEE), XIAORAN LIU[1], LEI ZHANG[2], AND JIBO WEI[1]

[1]College of Electronic Science and Technology, National University of Defense Technology, Changsha 410073, China
[2]School of Engineering, University of Glasgow, Glasgow G12 8QQ, U.K.

Corresponding author: Xiaoying Zhang (zhangxiaoying@nudt.edu.cn)

This work was supported by the Research Found of National University of Defense Technology under Grant ZK17-03-13.

ABSTRACT This paper devises a robust receiver for OFDM systems in the presence of residual timing offsets and unknown channel prior information. The proposed receiver constructs typical receiver models and resorts to the model selection technique to choose the best-matched receiver model to improve the channel estimation and signal detection. The typical receiver models are classified by considering the channel delay spread and the level of timing offset. Based on the receiver model selected by the Bayesian model selection algorithm, the channel length and timing offset parameters in the receiver model can provide the effective channel statistical information to make the channel estimator adapt to the altered circumstances and thus more accurate. Furthermore, the effective interference variance parameters in the selected receiver model are used to enhance the channel estimation and refine the soft symbol detection. The simulation results show that the proposed receiver achieves a significant performance gain compared to the existing methods. It is also shown that the proposed scheme makes the receiver robust to the diverse channel conditions and the timing offset states at a cost of the only a moderate increase in complexity.

INDEX TERMS Orthogonal frequency-division multiplexing (OFDM), channel estimation, symbol timing offset, model selection.

I. INTRODUCTION

Orthogonal frequency-division multiplexing (OFDM) is of great importance for modern wireless communication systems. The main advantages of OFDM systems include high spectral efficiency, low-complexity implementation, straightforward extension to Multiple Input Multiple Output (MIMO) and robustness against the frequency-selective channels with the high-efficiency one-tap equalizer [1]. OFDM systems also have some disadvantages, for example, OFDM is vulnerable to the synchronization errors. Although some new non-orthogonal waveforms, e.g., generalized frequency division multiplexing (GFDM), filter-bank multi-carrier (FBMC), etc., have been proved to be more robust to the synchronization errors [2], OFDM is still chosen as the base for the new radio of the 5G for the better backward-compatibility and technical maturity, according to the new technical specifications approved by the Third Generation Partnership Project (3GPP) [3]. To fulfill the various applications for the fifth-generation (5G) systems, some new challenges, e.g., diverse channel scenarios and non-ideal synchronization transmission need to be addressed for OFDM systems. With the increasing of diverse channel conditions and use cases, the receivers are required to achieve robust system performance over different channel models [4]. Specifically, to obtain the accurate channel state information for the coherent receiver, the channel estimator should cope with different channel delay spreads in general unknown wireless environments. On the other hand, 5G wireless communication systems will have to be able to support non-ideal synchronization transmissions in many use cases, e.g., machine type communications (MTC) and vehicular communications, where strict synchronization may not be supported by the limited power and overhead constraints. The residual timing offset due to the imperfect timing synchronization may affect the channel estimation (CE) and introduce inter-symbol interference (ISI) and inter-carrier interference (ICI) in the OFDM systems.

Channel estimation is a pivotal problem for OFDM systems. When the prior information of the channel, e.g., the power delay profile (PDP), is assumed to be known at the

The associate editor coordinating the review of this manuscript and approving it for publication was Gurkan Tuna.

receiver, the optimal channel estimation in terms of estimation mean square error (MSE) is linear minimum mean square error (MMSE) estimator. However, this assumption may not be achieved in the practical implementation, especially in complex propagation environments or when the channel conditions over which the communication systems operate are varying from one scenario to another. For instance, in the densely built urban areas or the hilly terrain environments, the propagation channels always have large multipath delay spread, while in the channels with line-of-sight (LOS) component, delay spread is much lower compared to the one in the non-line-of-sight (NLOS) scenarios. It is desirable to design a channel estimator which can adapt to various channel conditions. In literature, two commonly used methods have been considered to address the channel estimation when the prior information of channel is absence [5]–[7]. The first one is to apply the robust prior channel statistics to the channel estimator. This method is based on the facts that when the estimator is designed for the worst correlation, the statistical mismatch will be limited [5]. It has been proved in [6] that the uniform channel correlation matrix with the assumption that channel length equal to the cyclic prefix (CP) length L_{CP}, leads to robust CE performance. Besides the uniform correlation, exponential correlation property is also widely accepted since the first arrival channel paths are expected to contain larger power than the last paths. These methods have the merit of being simple, however, apparently suffer from performance loss when the practical channel length is much less than L_{CP}. To apply the bayesian CE, one can also resort to the channel statistical parameters estimation to obtain the prior information. In [8], the channel root-mean-square (RMS) delay spread is estimated based on the level-crossing rate of the channel frequency response. Average RMS delay spread of the channel is estimated in [9] by calculating the channel frequency correlation function. Hung etc. propose the PDP approximation method in [10] by estimating both the mean channel delay and the RMS delay spread. These methods need an extra effort for the parameters estimation in addition to the channel response estimation, which always lead to relatively high computational complexity to calculate the statistical expectation.

In OFDM systems, perfect symbol timing synchronization may not always be achieved, for example, in some machine type communications (MTCs) user cases, the synchronous requirement has to be relaxed due to the complexity and cost constraint. As a result, the residual symbol timing offset (STO) may always exists and thus need to be addressed to avoid the performance degradation. There are two possible cases for the OFDM systems with residual STO. In the first case, the orthogonality is still preserved thanks to the protection of CP. STO introduces a linear phase rotation which is proportional to the individual subcarrier index and can be absorbed to the channel frequency response (CFR). In this case, the residual STO can be compensated through the channel estimation and equalization theoretically [11]. However, the timing offset will shift the location of the effective channel impulse response (CIR) and thus make the channel estimation more challenging. In [12], the MMSE channel estimation is enhanced by considering both the channel statistics and the time offset statistics in the effective channel correlation function. However, the timing offset statistics may be affected by the channel properties and cannot be obtained beforehand in practice. In [13], the influence of STO on channel interpolation is analyzed and a compensation method for CE with STO is proposed. Besides the orthogonal case, the residual STO may introduce the ISI and ICI to the OFDM systems. Akaike information criterion has been used in [14], [15] to iteratively estimate the STO and CIR in time domain, however, these schemes requires many CE repetitions and additional fast Fourier Transforms (FFTs) and inverse FFTs (IFFTs) calculations, which lead to the high complexity burden.

To cope with the residual timing offset and the diverse channel conditions in the transmission scenario, a novel model classification-and-selection assisted robust receiver is proposed for OFDM systems in this paper. The contribution of this work consists of following aspects: first, we classify typical receiver models by considering both the channel lengths and the level of residual STOs. By using these receiver models, the abundant complicate channel parameters and STO value estimation can be avoided, while the channel delay spread matching the practical propagation environment and the state of the residual STO are taken into account in both the channel estimation and symbol detection. Second, an effective receiver model selection scheme is proposed to make the receiver adapt to its current channel condition and the level of STO with the best-matched model. Finally, by using the selected receiver model with both the effective channel prior information and the effective interference variance influenced by the residual STO, the proposed scheme can achieve superior system performance as compared to the traditional receivers. Since the proposed scheme preserves the core structure of the conventional channel estimation and soft detection, our design can be easily applied to the current and future multicarrier systems.

In the rest of the paper, we use $\boldsymbol{F}$ to denote an $N \times N$ FFT matrix with the (i,k)th entry $\boldsymbol{F}(i,k) = \exp\{-j2\pi ik/N\}$, $0 \le i \le N-1$, $0 \le k \le N-1$. $\bar{\mathbf{F}} = \boldsymbol{F}/\sqrt{N}$ is the $N \times N$ unitary FFT matrix. Superscripts $(\cdot)^T$ and $(\cdot)^H$ denote transpose and conjugate transpose, respectively. $[\cdot]_N$ refers to modulo N operation. diag($\boldsymbol{x}$) is a diagonal matrix with the diagonal elements taken from the vector $\boldsymbol{x}$. $\boldsymbol{I}_N$ is the $N \times N$ identity matrix and $\mathbf{0}_N$ is the $N \times 1$ vector with all the element being zero. We use $\mathcal{CN}(\boldsymbol{x}\,;\boldsymbol{a},\boldsymbol{\Sigma})$ to denote a vector $\boldsymbol{x}$ following the complex Gaussian distribution with the mean $\boldsymbol{a}$ and the covariance matrix $\boldsymbol{\Sigma}$.

II. RECEIVER WITH PERFECT SYNCHRONIZATION AND IDEAL CHANNEL

Let us consider an OFDM system with FFT length N. Among the N subcarriers, subcarriers with index set J_P are used to transmit N_P comb-type pilots for channel estimation, the subcarriers with index set J_D are assigned to transmit the N_D

user data. The transmitted pilot signal at the ith OFDM symbol is represented by the $N_P \times N_P$ diagonal matrix $\boldsymbol{\mathcal{X}}_i^P = \text{diag}\{[X_i(j_1), X_i(j_2), \cdots, X_i(j_{N_P})]\}$. The signal is transmitted through a frequency-selective fading channel, the channel impulse response (CIR) during the ith OFDM symbol can be expressed by the $N \times 1$ vector $\mathbf{h}_i = [h_i(0), h_i(1), \cdots, h_i(L_h - 1), 0, \cdots, 0]^T$, where $L_h - 1$ denotes the maximum delay spread and L_h represents the channel length. We assume $L_h \leq L_{CP} + 1$. The PDP of channel can be represented by the $N \times 1$ correlation vector $\mathbf{r}_h$ as

$$\mathbf{r}_h = \left[\delta_0^2\ \delta_1^2, \cdots, \delta_{L_h-1}^2, 0 \cdots 0\right]^T, \tag{1}$$

where $\delta_l^2 = E\{|h_i(l)|^2\}$, $0 \leq l \leq L_h - 1$. When the perfect synchronization is achieved, the received signal $\mathbf{Y}_i^P \in \mathcal{C}^{N_P \times 1}$ on the pilot subcarriers during the ith OFDM symbol can be written as

$$\mathbf{Y}_i^P = \boldsymbol{\mathcal{X}}_i^P \mathbf{F}_P \mathbf{h}_i + \mathbf{N}_i^P, \tag{2}$$

where $\mathbf{F}_P \in \mathcal{C}^{N_P \times N}$ is constructed by taking the rows of $\mathbf{F}$ with indices from J_P. $\mathbf{N}_i^P \in \mathcal{C}^{N_P \times 1}$ is the additive white Gaussian noise (AWGN) with covariance matrix $\boldsymbol{\Sigma}_n^P = \sigma_n^2 \mathbf{I}_{N_P}$, where σ_n^2 is the corresponding noise variance. Applying the LMMSE criterion with the a priori PDP (1), the CIR can be estimated as [7]

$$\hat{\mathbf{h}}_i = \Xi_h \mathbf{C}_i^H \left(\mathbf{C}_i \Xi_h \mathbf{C}_i^H + \boldsymbol{\Sigma}_n^P\right)^{-1} \mathbf{Y}_i^P, \tag{3}$$

where $\mathbf{C}_i = \boldsymbol{\mathcal{X}}_i^P \mathbf{F}_P$ is the $N_P \times N$ observation matrix and $\Xi_h = \text{diag}\{\mathbf{r}_h\}$ is the $N \times N$ channel correlation matrix. The CFR estimate can be calculated by $\hat{\mathbf{H}}_i = \mathbf{F}_D \hat{\mathbf{h}}_i$, where $\mathbf{F}_D \in \mathcal{C}^{N_D \times N}$ is formed by taking the rows of $\mathbf{F}$ with indices belonging to data subcarriers set J_D. For the kth data subcarrier, the frequency domain received signal can be written as

$$Y_i(k) = H_i(k) X_i(k) + N_i(k),\ k \in J_D, \tag{4}$$

where $X_i(k)$ and $H_i(k)$ are the transmitted signal and the CFR on the kth subcarrier, respectively. $N_i(k)$ is the frequency domain AWGN noise on the kth subcarrier with variance σ_n^2. Exploiting the CFR estimate $\hat{H}_i(k)$ on the kth subcarrier, i.e., the kth element of $\hat{\mathbf{H}}_i$, the soft demodulator calculates the log-likelihood ratios (LLR) of coded bits as follows [16]

$$L(b_{(i,k)}(j)) = \frac{1}{\sigma_n^2}\left[\min_{X_i(k) \in \beta_j^-} \left|Y_i(k) - \hat{H}_i(k) X_i(k)\right|^2 - \min_{X_i(k) \in \beta_j^+} \left|Y_i(k) - \hat{H}_i(k) X_i(k)\right|^2\right] \tag{5}$$

where $b_{(i,k)}(j)$ is the jth bit of $\mathbf{b}_{(i,k)}$ which is mapped to constellation symbol $X_i(k)$, $L(b_{(i,k)}(j))$ is the LLR of $b_{(i,k)}(j)$, β_j^- and β_j^+ denote the subset of constellation symbols with $b_{(i,k)}(j) = +1$ and $b_{(i,k)}(j) = -1$, respectively.

III. RECEIVER MODELS CONSTRUCTION

In this paper, we consider the case that symbol synchronization has been accomplished, while the residual STO still exists. Assume that the a priori correlation matrix of the channel is not known at the receiver. The receiver model construction consists of two steps, i.e., model classification and model parameters calculation. In the following, we first discuss the model classification based on the channel length and the timing offsets. Then, the parameters of the model, including the effective channel a priori correlation vector and the effective interference power affected by the STO, are derived.

A. MODEL CLASSIFICATION

The effective length of the channel and the residual STO are mutually coupled vital parameters for both the channel estimation and signal detection. However, in the diverse unknown channel conditions, accurate channel length estimation leads to high computational complexity, while the precise estimation for the residual STO may not be supported in the limited overhead and complexity constraint transmission scenario. In order to avoid the complicated procedures for the channel length and residual timing offset estimation, we choose to "quantize" a group of possible channel lengths/timing errors to the preset values according to their effect and then construct typical receiver models based on these preset values. For example, if the true channel length L_h and the timing offset θ are mapped to L_h^κ and θ^κ by the classifier, respectively. The model type M^κ with parameters L_h^κ and θ^κ is then adopted to the receiver. Here, the superscript κ denotes the type index for the receiver models.

For simplicity, an intuitive classification method is adopted here for the channel length and the residual STO, receptively. For the effective length of the channel, we classify the wireless channels into three types representing the short, medium, long multipath delay channels, respectively. Since we have assumed that $L_h \leq L_{CP} + 1$, the channel length of long-delay channel type is set as $L_{CP} + 1$, the channel length of the medium-delay channel type is approximately set as one half of the maximum delay, i.e., $L_{CP}/2$, and the short-delay type channel is assumed to have the length of $L_{CP}/4$, which is a half of the length of the medium-delay channel.

According to the influence of the timing error on the system model, the timing errors are classified into several typical states as well. Two main factors are considered for the classification in the STO domain. First, the residual STO will changes the effective channel response seen by the receiver. Second, the residual STO may introduce the ISI and ICI, which enhance the effective noise power of the receiver and thus affect the LLRs calculation of coded bits.

Suppose that the timing synchronization algorithm can limit the STO θ to a range $[-\theta_m, \theta_m]$ where θ_m is the positive maximum timing offset. The effective CIR $\mathbf{h}_i^\theta$ affected by a non-zero STO θ, is a cyclic-shifted version of the physical

TABLE 1. The receiver models.

STO domain \ Channel domain	$L_h^\kappa = L_{CP}/4$	$L_h^\kappa = L_{CP}/2$	$L_h^\kappa = L_{CP}+1$
$\theta^\kappa = -\theta_m$	Model I, M^{I}	Model II, M^{II}	Model III, M^{III}
$\theta^\kappa = -\theta_m/2$	Model IV, M^{IV}	Model V, M^{V}	Model VI, M^{VI}
$\theta^\kappa = 0$	Model VII, M^{VII}	Model VIII, M^{VIII}	Model IX, M^{IX}
$\theta^\kappa = \theta_m/2$	Model X, M^{X}	Model XI, M^{XI}	Model XII, M^{XII}
$\theta^\kappa = \theta_m$	Model XIII, M^{XIII}	Model XIV, M^{XIV}	Model XV, M^{XV}

channel $\mathbf{h}_i$ [12], e.g.,

$$h_i^\theta(l) = h_i([l-\theta]_N),\ 0 \le l \le N-1. \tag{6}$$

Naturally, the residual timing error θ can be divided into the right-side, left-side and null types [12], respectively.

When $\theta = 0$, the orthogonality of OFDM system is preserved. In this case, channel properties only depend on the physical propagation environment and there is no extra interference in frequency domain. When $\theta < 0$, the STO belongs to the right-side type, e.g., the estimated starting point is later than the proper timing instance. In this case, the effective CIR is a cyclic-shifted version of $\mathbf{h}_i$ with a leftward shifting length $|\theta|$. At the same time, the ISI is incurred by introducing the $|\theta|$ data points of the next OFDM symbol. To represent different cyclic shifts of the channel and distinguish interference power with different levels, we subdivide $\theta < 0$ type into two secondary classes with $\theta = -\theta_m/2$ and $\theta = -\theta_m$, respectively. For the left-side type STO with $\theta > 0$, the estimated starting point is earlier than the proper timing instance. In this case, the effective CIR is a cyclic-shifted version of $\mathbf{h}_i$ with a rightward shifting length $|\theta|$. To represent different cyclic shifts of the channel, we also subdivide $\theta > 0$ type STO into two secondary classes with $\theta = \theta_m/2$ and $\theta = \theta_m$, respectively. As will be shown in the Section V, when $\theta > 0$, the effective interference level may be zero or relatively small due to the protection of CP, thus the effect on the effective channel length is the main consideration to classify the secondary classes.

Combined the timing offsets states with three channel length types, the receiver models M^κ, $\kappa \in \{\mathrm{I,II},\ldots,\mathrm{XV}\}$, are obtained in Table 1. Note that the classification scheme used here is intuitive and mainly designed for reducing the additional complexity. The number of receiver model types, the coupled "quantized" parameter vector $(L_h^\kappa, \theta^\kappa)$ and its corresponding input range of (L_h, θ) may be optimized from different perspectives. If the corresponding complexity is affordable, more sophisticated schemes and models can be adopted. For example, we can increase the number of model types with different $(L_h^\kappa, \theta^\kappa)$ for better resolution of the channel length and timing offset at the cost of larger complexity. Besides the channel classification scheme we used here, from the perspective of channel propagation scenarios, different channel models defined in the communication standards [17], e.g., Extended Pedestrian A model (EPA) or Extended Vehicular A model (EVA) etc. can also be used as the candidate channel types, which are further combined with the residual STO states to construct receiver models.

B. MODEL PARAMETERS CALCULATION

To make the receiver adaptive to the diverse propagation scenarios and different timing offsets, the effective a priori PDP of channel and effective interference variance are calculated for each receiver model.

For arbitrary receiver model $M^\kappa, \kappa \in \{\mathrm{I},\cdots,\mathrm{XV}\}$, we can directly read the "quantized" representative channel length L_h^κ and timing offset θ^κ from Table 1. With L_h^κ and θ^κ, the effective channel correlation vector $\mathbf{r}_\kappa$ for the receiver model M^κ can be calculated by using the robust exponentially decaying multipath PDP [7] as

$$\mathbf{r}_\kappa(l) = \tilde{\mathbf{r}}_\kappa(\left[l-\theta^\kappa\right]_N),\ 0 \le l \le N-1, \tag{7}$$

with

$$\tilde{\mathbf{r}}_\kappa(l) = \begin{cases} e^{-j\frac{\ln(2L_h^\kappa)}{L_h^\kappa}} \Big/ \sum_{n=0}^{L_h^\kappa-1} e^{-n\frac{\ln(2L_h^\kappa)}{L_h^\kappa}}, \\ \qquad 0 \le l \le L_h^\kappa - 1 \\ 0, \\ \qquad L_h^\kappa \le l \le N-1 \end{cases}. \tag{8}$$

Next we discuss the effective frequency-domain interference variance.

For M^κ, $\kappa \in \{\mathrm{VII,VIII,IX}\}$, with $\theta^\kappa = 0$, since the orthogonality among subcarriers is preserved, the effective frequency-domain interference variance vector $\boldsymbol{\mathcal{I}}^\kappa = \mathbf{0}_N$. For M^κ, $\kappa \in \{\mathrm{I},\cdots,\mathrm{VI}\}$, with $\theta^\kappa < 0$. The frequency-domain interference is incurred by the ISI from the next OFDM symbol. Let us consider the system model with residual STO $\theta^\kappa < 0$. For convenience, we neglect the channel variation between consecutive OFDM symbols. Assume that the time-domain transmitted signal during the ith symbol is $\mathbf{x}_i = [x_i(0), x_i(1), \cdots, x_i(N-1)]^T$, the time-domain received signal vector $\mathbf{y}_i \in \mathcal{C}^{N\times 1}$ can be written as

$$\mathbf{y}_i = \boldsymbol{H}_i^{\theta^\kappa}\mathbf{x}_i - \mathbf{A}\mathbf{x}_i + \mathbf{B}\mathbf{x}_{i+1} + \mathbf{n}_i \tag{9}$$

where $\boldsymbol{H}_i^{\theta^\kappa}$ is an $N\times N$ cyclic matrix whose first column is $\mathbf{h}_i^{\theta^\kappa}$ with $\mathbf{h}_i^{\theta^\kappa}(l) = \mathbf{h}_i([l-\theta^\kappa]_N)$, $0 \le l \le N-1$. The term $-\mathbf{A}\mathbf{x}_i$ is added for constructing the cyclic matrix $\boldsymbol{H}_i^{\theta^\kappa}$, $\mathbf{A}$ is an $N\times N$ matrix with elements given by $\mathbf{A}(d,j) = h_i(d-j-N-\theta^\kappa)$. $\mathbf{B}\mathbf{x}_{i+1}$ is the ISI term incurred by the $(i+1)$th symbol with $\mathbf{B}(d,j) = h_i(d-[j+L_{CP}]_N-N-\theta^\kappa)$, which is obtained by cyclic shifting the columns of $\mathbf{A}$ to the left by L_{CP}. $\mathbf{n}_i \in \mathcal{C}^{N\times 1}$ is the AWGN term with each entry having variance of σ_n^2.

Multiplying both sides of (9) by $\bar{\mathbf{F}}$, the frequency domain received signal $\mathbf{Y}_i \in \mathcal{C}^{N\times 1}$ can be written as

$$\mathbf{Y}_i = \boldsymbol{\mathcal{X}}_i \mathbf{F}\mathbf{h}_i^{\theta^\kappa} + \mathbf{W}_i^{\theta^\kappa} + \mathbf{N}_i, \tag{10}$$

where $\boldsymbol{\mathcal{X}}_i = \text{diag}([X_i(0), X_i(1), \cdots, X_i(N-1)]^T)$ is the ith frequency-domain transmitted symbol with $X_i(n)$ being the transmitted signal on the nth subcarrier. $\mathbf{N}_i$ is the frequency domain AWGN noise, $\mathbf{W}_i^{\theta^\kappa} = \bar{\mathbf{F}}(-\mathbf{A}\mathbf{x}_i + \mathbf{B}\mathbf{x}_{i+1})$ is the $N\times 1$ frequency domain interference vector with the kth entry being

$$\begin{aligned} W_i^{\theta^\kappa}(k) = &-\frac{1}{N}\sum_{n=0}^{N-1}\sum_{m=0}^{-\theta^\kappa-1}\sum_{d=N+\theta^\kappa+m}^{N-1} h_i(m)e^{-j\frac{2\pi}{N}(k-n)d} \\ &\times e^{-j\frac{2\pi}{N}(m+\theta^\kappa)n}X_i(n) \\ &+\frac{1}{N}\sum_{n=0}^{N-1}\sum_{m=0}^{-\theta^\kappa-1}\sum_{d=N+\theta^\kappa+m}^{N-1} h_i(m)e^{-j\frac{2\pi}{N}(k-n)d} \\ &\times e^{-j\frac{2\pi}{N}(m+\theta^\kappa+L_{CP})n}X_{i+1}(n) \end{aligned} \tag{11}$$

Assume that the complex channel path gains $\{h_i(m)\}$ are uncorrelated and the transmitted symbols $\{X_i(n)\}$ are mutually independent random variables with zero means and equal power σ_x^2. The power of the frequency-domain interference $W_i^{\theta^\kappa}(k)$, $0 \le k \le N-1$, can be written as

$$\boldsymbol{\mathcal{I}}^\kappa(k) = \frac{2\sigma_x^2}{N^2}\sum_{m=0}^{-\theta^\kappa-1}\tilde{\mathbf{r}}_\kappa(m)\sum_{n=0}^{N-1}\left|\sum_{d=N+\theta^\kappa+m}^{N-1} e^{-j\frac{2\pi}{N}(k-n)d}\right|^2, \tag{12}$$

where $\boldsymbol{\mathcal{I}}^\kappa \in \mathcal{C}^{N\times 1}$ is the interference power vector. From (12), we can see that the power of interference depends on the correlation function of the CIR and the residual STO θ^κ. Since each summation term in (11) is zero-mean, we approximately regard $W_i^{\theta^\kappa}(k)$ as effective Gaussian noise with zero mean and variance $\boldsymbol{\mathcal{I}}^\kappa(k)$ to improve the channel estimation and signal detection.

For M^κ, $\kappa \in \{\text{X}, \cdots, \text{XV}\}$, with $\theta^\kappa > 0$, if the condition $\theta^\kappa + L_h^\kappa > L_{CP}+1$ is satisfied, ISI is incurred by the previous symbol. In this case, the time domain received signal vector $\mathbf{y}_i$ can be written as

$$\mathbf{y}_i = \boldsymbol{H}_i^{\theta^\kappa}\mathbf{x}_i - \bar{\mathbf{A}}\mathbf{x}_i + \bar{\mathbf{B}}\mathbf{x}_{i-1} + \mathbf{n}_i, \tag{13}$$

In (13), $\boldsymbol{H}_i^{\theta^\kappa}$ is an $N\times N$ cyclic matrix with the first column being $\mathbf{h}_i^{\theta^\kappa}$. $-\bar{\mathbf{A}}\mathbf{x}_i$ is added for constructing the cyclic matrix, where $\bar{\mathbf{A}}$ is an $N\times N$ matrix with elements given by $\bar{\mathbf{A}}(d,j) = h_i(d-[j+L_{CP}]_N + N + L_{CP} - \theta^\kappa)$. $\bar{\mathbf{B}}\mathbf{x}_{i-1}$ is the ISI term incurred by the $(i-1)$th symbol with $\bar{\mathbf{B}}(d,j) = h_i(d-j+N+L_{CP}-\theta^\kappa)$. Note that matrix $\bar{\mathbf{A}}$ can be obtained by cyclic shifting the columns of $\bar{\mathbf{B}}$ to the left by L_{CP}. $\mathbf{n}_i$ is the AWGN term. Similarly to (10), after transforming $\mathbf{y}_i$ in (13) into the frequency domain, the frequency domain received signal $\mathbf{Y}_i$ can also be decomposed into the desired signal term $\boldsymbol{\mathcal{X}}_i\mathbf{F}\mathbf{h}_i^{\theta^\kappa}$, the AWGN term and the effective interference vector $\mathbf{W}_i^{\theta^\kappa} = \bar{\mathbf{F}}(-\bar{\mathbf{A}}\mathbf{x}_i + \bar{\mathbf{B}}\mathbf{x}_{i-1})$. The k-th entry of $\mathbf{W}_i^{\theta^\kappa}$ can be written as

$$\begin{aligned} W_i^{\theta^\kappa}(k) = &-\frac{1}{N}\sum_{n=0}^{N-1}\sum_{m=L_{CP}-\theta^\kappa+1}^{L_h-1}\sum_{d=0}^{m-L_{CP}+\theta^\kappa-1} h_i(m) \\ &\times e^{-j\frac{2\pi}{N}(k-n)d}e^{-j\frac{2\pi}{N}(m+\theta^\kappa)n}X_i(n) \\ &+\frac{1}{N}\sum_{n=0}^{N-1}\sum_{m=L_{CP}-\theta^\kappa+1}^{L_h-1}\sum_{d=0}^{m-L_{CP}+\theta^\kappa-1} h_i(m) \\ &\times e^{-j\frac{2\pi}{N}(k-n)d}e^{-j\frac{2\pi}{N}(m+\theta^\kappa-L_{CP})n}X_{i-1}(n) \end{aligned} \tag{14}$$

The effective interference variance on the kth subcarrier can be written as

$$\boldsymbol{\mathcal{I}}^\kappa(k) = \frac{2\sigma_x^2}{N^2}\sum_{m=L_{CP}-\theta^\kappa+1}^{L_h-1}\tilde{\mathbf{r}}_\kappa(m)\sum_{n=0}^{N-1}\left|\sum_{d=0}^{m-L_{CP}+\theta^\kappa-1} e^{-j\frac{2\pi}{N}(k-n)d}\right|^2, \tag{15}$$

For M^κ with $\kappa = \{\text{X}, \cdots, \text{XV}\}$ and $\theta^\kappa > 0$, if $\theta^\kappa + L_h^\kappa \le L_{CP}+1$, the power of $W_i^{\theta^\kappa}(k)$ degenerates to zero, since θ^κ is in the ISI-free region of CP.

In a nutshell, the following receiver models and model parameters are obtained for the proposed receive scheme.

1) According to the propagation channel conditions and the timing offset states, the receiver model set consists of $Q = 15$ models, e.g., $M^\kappa = \{\mathbf{r}_\kappa, \boldsymbol{\mathcal{I}}^\kappa\}$, $\kappa = \{\text{I}, \cdots, XV\}$, where $\mathbf{r}_\kappa$ is the effective channel correlation vector given by (7) and $\boldsymbol{\mathcal{I}}^\kappa$ is the effective frequency domain interference variance vector.

2) For M^κ with $\kappa \in \{\text{I}, \cdots, \text{VI}\}$, the effective interference variance matrix $\boldsymbol{\mathcal{I}}^\kappa$ can be derived by (12); For M^κ with $\kappa = \{\text{VII}, \cdots, \text{IX}\}$ and M^κ with $\kappa \in \{\text{X}, \cdots, \text{XV}\}$ satisfying $\theta^\kappa + L_h^\kappa \le L_{CP}+1$, there is no additional interference, e.g., $\boldsymbol{\mathcal{I}}^\kappa = \mathbf{0}_N$; For M^κ with $\kappa \in \{\text{X}, \cdots, \text{XV}\}$ satisfying $\theta^\kappa + L_h^\kappa > L_{CP}+1$, each element of $\boldsymbol{\mathcal{I}}^\kappa$ is calculated by (15).

Note that we can adaptively set Q to achieve the tradeoff between the diverse physical channel scenarios, STO states and the computational complexity.

IV. MODEL SELECTION ASSISTED RECEIVER

In this Section, we discuss how to select the matched receiver model to improve the channel estimator and soft demodulation. In order to pick the appropriate receiver model in a cost-effective manner, we invoke the Bayesian Model Selection (BMS) approach [18] based on the pilot symbols transmitted for channel estimation. Based on (2) and (10), the received signal on the pilot subcarriers $\mathbf{Y}_i^P$ affected by the residual STO θ can be rewritten as

$$\mathbf{Y}_i^P = \mathbf{C}_i\mathbf{h}_i^\theta + \bar{\mathbf{W}}_i^P, \tag{16}$$

where $\bar{\mathbf{W}}_i^P = \mathbf{W}_i^{\theta,P} + \mathbf{N}_i^P$ is the effective frequency domain noise on the pilot subcarriers including both the AWGN $\mathbf{N}_i^P$ and the interference $\mathbf{W}_i^{\theta,P} \in \mathcal{C}^{N_P\times 1}$ incurred by the STO.

$\mathbf{W}_i^{\theta,P}$ is constructed by taking rows of $\mathbf{W}_i^{\theta}$ with indices from J_P, the elements of $\mathbf{W}_i^{\theta}$ can be calculated by (11) or (14). Assume that we use the comb-type pilots in the N_s OFDM symbols to select the receiver model. According to the BMS criteria, the receiver model with the maximum a posteriori probability should be picked as the matched model. Since there is no priori information for receiver model, the model is selected by maximizing the joint log-likelihood function $\ln\prod_{i=1}^{N_s} p(\mathbf{Y}_i^P|M^\kappa)$ as

$$\begin{aligned}\gamma &= \arg\max_{\kappa=\mathrm{I},\cdots,\mathrm{XV}} \ln\prod\nolimits_{i=1}^{N_s} p(\mathbf{Y}_i^P|M^\kappa)\\ &= \arg\max_{\kappa=\mathrm{I},\cdots,\mathrm{XV}} \sum_{i=1}^{N_s} \ln\int p(\mathbf{Y}_i^P|\mathbf{h}_i^\theta, M^\kappa)p(\mathbf{h}_i^\theta|M^\kappa)d\mathbf{h}_i^\theta\\ &= \arg\max_{\kappa=\mathrm{I},\cdots,\mathrm{XV}} \sum_{i=1}^{N_s} -\ln\left(\left|\mathbf{\Omega}_i^\kappa\right|\right) - (\mathbf{Y}_i^P)^H(\mathbf{\Omega}_i^\kappa)^{-1}\mathbf{Y}_i^P, \end{aligned} \tag{17}$$

where $p(\mathbf{Y}_i^P|\mathbf{h}_i^\theta, M^\kappa) = \mathcal{CN}(\mathbf{Y}_i^P; \mathbf{C}_i\mathbf{h}_i^\theta, \Sigma_\kappa^P)$ is based on system model (16) with the effective noise covariance matrix $\Sigma_\kappa^P = \mathrm{diag}\{\left[\boldsymbol{\mathcal{I}}^\kappa(j_1)+\sigma_n^2, \boldsymbol{\mathcal{I}}^\kappa(j_2)+\sigma_n^2, \cdots, \boldsymbol{\mathcal{I}}^\kappa(j_{N_P})+\sigma_n^2\right]^T\}$. Note that both the AWGN noise variance and effective frequency domain interference variance are taken into account in Σ_κ^P. $p(\mathbf{h}_i^\theta|M^\kappa) = \mathcal{CN}(\mathbf{h}_i^\theta; \mathbf{0}_N, \Xi_\kappa)$ with $\Xi_\kappa = \mathrm{diag}(\mathbf{r}_\kappa)$ represents the a priori correlation vector for the effective CIR $\mathbf{h}_i^\theta$ effected by the STO θ. By using $\int p(\mathbf{Y}_i^P|\mathbf{h}_i^\theta, M^\kappa)p(\mathbf{h}_i^\theta|M^\kappa)d\mathbf{h}_i^\theta = \mathcal{CN}(\mathbf{Y}_i^P; \mathbf{0}_N, \Omega_i^\kappa)$, $\Omega_i^\kappa = \Sigma_\kappa^P + \mathbf{C}_i\Xi_\kappa\mathbf{C}_i^H$ can be calculated accordingly.

Based the selected receiver model M^γ, the model parameters $M^\gamma = \left\{\mathbf{r}_\gamma, \boldsymbol{\mathcal{I}}^\gamma\right\}$ are used to make the receiver work in the right state. From (16), one can see that since we approximate the interference as the effective Gaussian noise, the LMMSE channel estimator given by (3) can be directly extended to estimate effective channel impulse response $\hat{\mathbf{h}}_i^\theta$ as

$$\hat{\mathbf{h}}_i^\theta = \Xi_\gamma\mathbf{C}_i^H\left(\mathbf{C}_i\Xi_\gamma\mathbf{C}_i^H + \Sigma_\gamma^P\right)^{-1}\mathbf{Y}_i^P. \tag{18}$$

In (18), $\Sigma_\gamma^P = \mathrm{diag}\{\left[\boldsymbol{\mathcal{I}}^\gamma(j_1)+\sigma_n^2, \cdots, \boldsymbol{\mathcal{I}}^\gamma(j_{N_P})+\sigma_n^2\right]^T\}$ is the effective frequency domain noise covariance matrix for the pilot subcarriers. $\Xi_\gamma = \mathrm{diag}(\mathbf{r}_\gamma)$ is the effective a priori channel correlation matrix.

Similarly, based on (10), the frequency domain received signal for the k-th data subcarrier with the residual STO θ can be written as

$$Y_i(k) = H_i^\theta(k)X_i(k) + \bar{W}_i(k), k \in J_D, \tag{19}$$

where $\bar{W}_i(k) = W_i^\theta(k) + N_i(k)$ is the zero-mean effective frequency domain noise on the kth subcarrier. $W_i^\theta(k)$ represents the possible interference term induced by the residual STO, the variance of $W_i^\theta(k)$ can be approximated by $\boldsymbol{\mathcal{I}}^\gamma(k)$ with the selected receiver model M^γ. $H_i^\theta(k)$ denote the effective CFR on the kth subcarriers affected by the STO θ. The soft demodulation given by (5) can also be applied to system model (19) as [16]

$$L(b_{(i,k)}(j)) = \frac{1}{\sigma^2(k)}\left[\min_{X_i(k)\in\beta_j^-}\left|Y_i(k) - \hat{H}_i^\theta(k)X_i(k)\right|^2 - \min_{X_i(k)\in\beta_j^+}\left|Y_i(k) - \hat{H}_i^\theta(k)X_i(k)\right|^2\right], \tag{20}$$

where $\hat{H}_i^\theta(k)$ is the kth element of the frequency domain effective CFR $\hat{\mathbf{H}}_i^\theta = \mathbf{F}_D\hat{\mathbf{h}}_i^\theta$, $\sigma^2(k) = \boldsymbol{\mathcal{I}}^\gamma(k) + \sigma_n^2$ denotes the effective noise on the kth data subcarrier, which considers both the AWGN variance σ_n^2 and the effective frequency domian interference variance $\boldsymbol{\mathcal{I}}^\gamma(k)$.

We briefly evaluate the computational complexity of the proposed scheme. The proposed receiver consists of three main stages, e.g., model construction, model selection, channel estimation and soft demodulation. Note that the model construction stage can be performed off-line and the model parameters can be pre-calculated and stored in the receiver beforehand. The channel estimator and soft demodulation share the same structures with the traditional receiver. Therefore, here we focus on the on-line additional computational complexity required by the model selection stage. We assume that the same pilot symbols are used for the N_s OFDM symbols to select the receiver model. For Q preset receiver models, the joint log-likelihood function needs Q inversions of $N_P \times N_P$ matrix Ω_i^κ and Q logarithmic determinant calculations for Ω_i^κ, each matrix inversion or determinant calculation requires $\mathcal{O}(N_P^3)$ operations [19]. In addition, the calculation of (17) requires $QN_s(N_P^2 + N_P) + QN_PL_{CP}(N_P + 1/2)$ complex multiplications (CM) and $QN_s(N_P-1)(N_P+1)+QN_P(L_{CP}-1)(N_P - 1/2)$ complex additions (CA).

V. SIMULATION RESULTS

In this section, the performance of the proposed robust receiver is evaluated with simulations. An OFDM system with $N = 512$, $L_{CP} = 128$ and a bandwidth of 8 MHz is considered. Among the N subcarriers, the 408 subcarriers in the middle of spectrum except the direct-current subcarrier are used to transmit the useful signals. The frequency-domain comb-type pilot subcarriers spacing is 4, the Zadoff-Chu sequences [20] with root index 23 are generated for the 102 pilot symbols inserted in each OFDM symbol. For channel coding, a half-rate convolutional code with encoding polynomials $(7, 5)_8$ is considered. The data symbols are modulated using the quadrature phase shift keying (QPSK) constellation.

A. THE INTERFERENCE ANALYSIS

FIGURE 1 compares the simulated interference power and the analytical interference power versus subcarrier indexes with different STOs. In this study, the analytical interference power is calculated by (12) and (15) in Section III. The exponential decay PDP channel model with $L_h = L_{CP}$ is considered. It can be seen in FIGURE 1 that there is a good match between the theoretical interference power and the numerical

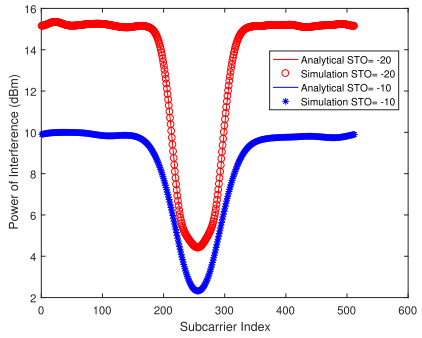

(a) Interference power with $\theta = -20$ and $\theta = -10$.

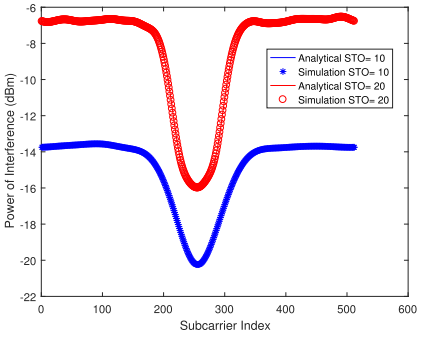

(b) Interference power with $\theta = 20$ and $\theta = 10$.

FIGURE 1. **Interference power analysis for different STO values.**

one in different cases with STO $\theta = -20, -10, 10, 20$, respectively, which validates our analysis in Section III. It is also observed that as the absolute value of STOs increases, the interference power increases accordingly. With the same absolute value of STO, the interference power with negative STO is larger than that with the positive ones due to the protection of CP. We can also find in FIGURE 1 that the data subcarriers near the virtual subcarriers, e.g., subcarriers 206-308, suffer less interference, which enlighten us to distinguish the interference power on different subcarriers.

B. RECEIVER PERFORMANCE

In this subsection, we compare the bit error rate (BER) for different receivers to evaluate the performance of the proposed receiver. Here the "Proposed 15 Models" refers to the proposed robust receiver with 15 models listed in Table 1. The "Proposed 9 Models" has 9 receiver models constructed by the combination of three possible channel lengths, e.g., $L_h^\kappa = L_{CP}/4, L_{CP}/2, L_{CP}+1$ and three possible STOs, e.g., $\theta^\kappa = -\theta_m, 0, \theta_m$. The comb-type pilots on the $N_s = 5$ OFDM symbols are used to select the matched receiver models for both "Proposed 15 Models" and "Proposed 9 Models" schemes. "Enhanced MMSE" refers to the improved receiver proposed by [12]. The "Conventional Receiver" neglects the residual STO and applies the robust exponential PDP [7] with $L_h = (L_{CP}+1)$ to channel estimation. The "Ideal performance" refers to the ideal receiver with zero-STO and the perfectly known channel PDP, which is the benchmark for comparison.

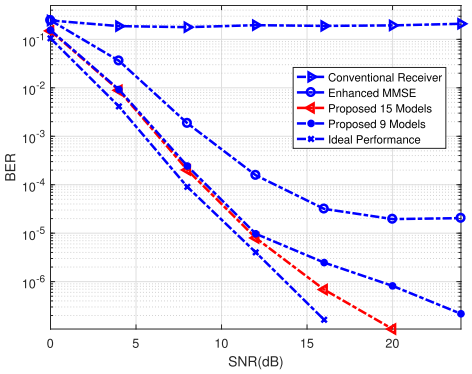

FIGURE 2. **BER performance versus SNR with the EVA channel and $\theta \in [-10, 10]$.**

In FIGURE 2, we compare the BER performance of difference receives. Here, the physical channel is characterized by the Extended Vehicular A model (EVA) channel model [17], the residual STO is assumed to be uniformly distributed over $[-10, 10]$. It can be observed that the proposed 15 models receiver has a better performance than the conventional receiver and the enhanced MMSE receiver. When BER $= 10^{-4}$, the proposed 15 models selection receiver offers about 4.5 dB gain than the enhanced MMSE receiver. Throughout the simulated range of SNRs, the conventional receiver doesn't work well because it neglects the effect of STO and roughly guess the channel to be an exponential-decaying $(L_{CP}+1)$-length channel. It can be found that the proposed 15 models selection receiver has less than 2 dB loss compared to the ideal receiver when BER $= 10^{-6}$. We can infer that this performance loss exists because we just classify the residual STOs and the channel lengths to the typical models to avoid solving estimation problems for all the related parameters. It can also be seen that the proposed 15 models receiver performs nearly the same with the 9 models selection receiver when SNR < 12 dB. This phenomenon gives us an insight that if the receiver works in the medium or low SNR region with a mildly time-dispersive channel and moderate residual STOs, we can reduce the model number to achieve better tradeoff between the performance and complexity. Besides the EVA channel model, the BER performances are evaluated and compared for different receivers under the Extended Typical Urban (ETU) channel model [17] with the residual STO uniformly distributed over $[-20, 20]$ in FIGURE 3. Similarly, it can be seen in FIGURE 3 that the enhanced MMSE receiver scheme exhibits an error floor. Both the proposed 15 models selection receiver and 9 models selection receiver achieve significant performance gains relative to the conventional receiver and the enhanced MMSE receiver. When BER $= 10^{-6}$, the performance gap between the ideal receiver and the proposed 15 models selection receiver is approximately 1.5 dB. These results validate the robustness of the proposed receiver to the practical channel PDPs.

In FIGURE 4, we compare the BER performance of difference receivers under the long-delay channel with the

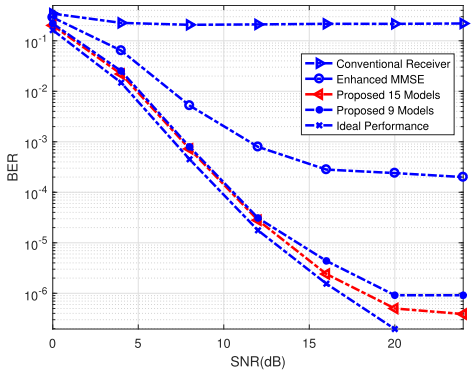

FIGURE 3. BER performance versus SNR with the ETU channel and $\theta \in [-20, 20]$.

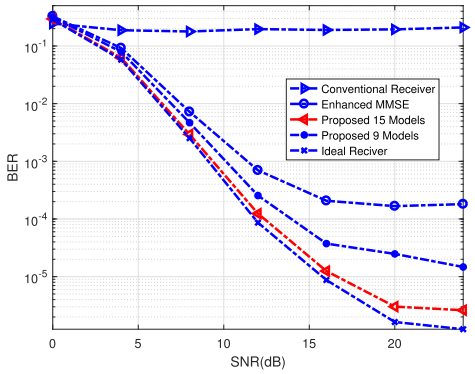

FIGURE 4. BER performance versus SNR with the exponential decaying channel and $\theta \in [-20, 20]$.

exponential decaying PDP and $L_h = L_{CP} + 1$. The residual STO has discrete uniform distribution over $[-20, 20]$. Again, it can be observed that the proposed 15 models receiver can effectively improve the system performance in terms of BER compared to the conventional receiver and the enhanced MMSE receiver. At a BER of 10^{-3}, the proposed 15 models selection receiver yields a performance gain of about 2.5 dB compared to the enhanced MMSE receiver. When BER $= 10^{-5}$, the performance gap between the ideal receiver and the proposed 15 model selection receive is less than 1 dB. We observe that the performance of the proposed 9 models selection receiver is significantly improved by the 15 models one, which verify that the performance of the proposed receiver scheme can be improved by increasing the number of the receiver models to distinguish the receiver states more precisely.

C. THE CORRECT MODEL SELECTION RATIO

As shown in FIGURE 5, we plot the successful model selection performance as a function of SNR for different number of pilot symbols. Here, the channel is exponentially decaying channel with $L_h = L_{CP}/4$ and the STO is set to be zero. The correct model selection probability is defined as the average ratio of correctly identifying the right model. In this case, the right receiver model is Model VII in Table 1. As expected, the correct model selection probability is monotonically

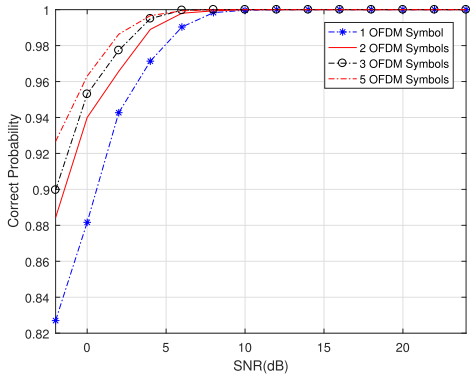

FIGURE 5. The correct model selection probability versus SNR.

increased as the SNR values or the OFDM symbols used for model selection increases. It can be noted that the proposed model classification-and-selection receiver can share the pilot symbols assigned for channel estimation, and thus do not need extra overhead specially.

VI. CONCLUSION

In this paper, we propose a model classification-and-selection assisted robust receiver for OFDM systems with residual STOs. We first classify typical receiver models according to the length of the channel and the level of the timing error. In each receiver model, the effective a priori channel correlation vector is calculated by considering the cyclic shift of the effective channel CIR with residual STOs. Meanwhile, the effective frequency domain interference power is analyzed to measure the enhancement of the noise floor due to the STOs for each subcarrier. A bayesian model selection algorithm is derived by using the pilot symbols inserted in the OFDM symbols, which chooses the best matched model and output the corresponding model parameters to assist the channel estimation and soft demodulation. Various numerical and simulation results are given to show the effectiveness of the proposed algorithms. We highlight that the proposed receiver scheme can be easily extend to the current and future multicarrier systems based on OFDM, which greatly enhance the receiver robustness against the diverse channel conditions and non-ideal synchronization transmission scenarios.

REFERENCES

[1] Y. S. Cho, J. Kim, W. Y. Yang, and C. G. Kang, *MIMO-OFDM Wireless Communications with MATLAB*. Hoboken, NJ, USA: Wiley, 2010, pp. 115–131.

[2] B. Lim and Y.-C. Ko, "SIR analysis of OFDM and GFDM waveforms with timing offset, CFO, and phase noise," *IEEE Trans. Wireless Commun.*, vol. 16, no. 10, pp. 6979–6990, Oct. 2017.

[3] *Technical Specification Group Radio Access Network; nr; Physical Channels and Modulation, Version 15.1.0*, document 38, 211, 3GPP, Mar.2018.

[4] Z. E. Ankarali and B. Peköz, and H. Arslan, "Flexible radio access beyond 5G: A future projection on waveform, numerology, and frame design principles," *IEEE Access*, vol. 5, pp. 18295–18309, 2017.

[5] O. Edfors, M. Sandell, J. J. van de Beek, S. K. Wilson, and P. O. Börjesson, "OFDM channel estimation by singular value decomposition," *IEEE Trans. Commun.*, vol. 46, no. 7, pp. 931–939, Jul. 1998.

[6] Y. Li, "Pilot-symbol-aided channel estimation for OFDM in wireless systems," *IEEE Trans. Veh. Technol.*, vol. 49, no. 4, pp. 1207–1215, Jul. 2000.

[7] Y. Liu, Z. Tan, H. Hu, L. J. Cimini, and G. Y. Li, "Channel estimation for OFDM," *IEEE Commun. Surveys Tuts.*, vol. 16, no. 4, pp. 1891–1908, 4th Quart., 2014.

[8] K. Witrisal, Y.-H. Kim, and R. Prasad, "A new method to measure parameters of frequency-selective radio channels using power measurements," *IEEE Trans. Commun.*, vol. 49, no. 10, pp. 1788–1800, Oct. 2001.

[9] T. Yucek and H. Arslan, "Time Dispersion and Delay Spread Estimation for Adaptive OFDM Systems," *IEEE Trans. Veh. Technol.*, vol. 57, no. 3, pp. 1715–1722, May 2008.

[10] K.-C. Hung and D. W. Lin, "Pilot-based LMMSE channel estimation for OFDM systems with power–delay profile approximation," *IEEE Trans. Veh. Technol.*, vol. 59, no. 1, pp. 150–159, Jan. 2010.

[11] M. Speth, S. Fechtel, G. Fock, and H. Meyr, "Optimum receiver design for OFDM-based broadband transmission.II. A case study," *IEEE Trans. Commun.*, vol. 49, no. 4, pp. 571–578, Apr. 2001.

[12] C. R. N. Athaudage and A. D. S. Jayalath, "Enhanced MMSE channel estimation using timing error statistics for wireless OFDM systems," *IEEE Trans. Broadcast.*, vol. 50, no. 4, pp. 369–376, Dec. 2004.

[13] D.-C. Chang, "Effect and compensation of symbol timing offset in OFDM systems with channel interpolation," *IEEE Trans. Broadcast.*, vol. 54, no. 4, pp. 761–770, Dec. 2008.

[14] E. G. Larsson, G. Liu, J. Li, and G. B. Giannakis, "Joint symbol timing and channel estimation for OFDM based WLANs," *IEEE Commun. Lett.*, vol. 5, no. 8, pp. 325–327, Aug. 2001.

[15] A. Tomasoni, D. Gatti, S. Bellini, M. Ferrari, and M. Siti, "Efficient OFDM channel estimation via an information criterion," *IEEE Trans. Wireless Commun.*, vol. 12, no. 3, pp. 1352–1362, Mar. 2013.

[16] X. Zhang, L. Zhang, P. Xiao, D. Ma, J. Wei, and Y. Xin, "Mixed numerologies interference analysis and inter-numerology interference cancellation for windowed OFDM systems," *IEEE Trans. Veh. Tech.*, vol. 67, no. 8, pp. 7047–7061, Apr. 2018.

[17] *Evolved Universal Terrestrial Radio Access (E-UTRA); User Equipment (UE) Radio Transmission and Reception*, document 3GPP Specification 36.101, Technical Specification Group Radio Access Network, 2010.

[18] T. Soderstrom and P. Stoica, *System identification*, 1st ed. Upper Saddle River, NJ, USA: Prentice-Hall, 1989.

[19] V. S. Ryaben'kii and S. V. Tsynkov, *A Theoretical Introduction to Numerical Analysis*. Boca Raton, FL, USA: CRC Press, 2006.

[20] D. Chu, "Polyphase codes with good periodic correlation properties," *IEEE Trans. Inf. Theory*, vol. IT-18, no. 4, pp. 531–532, Jul. 1972.

XIAOYING ZHANG received the M.S. and Ph.D. degrees in communication engineering from the National University of Defense Technology (NUDT), Changsha, China, in 2002 and 2008, respectively. From 2007 to 2008, she was a Visiting Scholar with Kyushu University, Japan. Since 2014, she has been an Associate Professor with NUDT. In 2017, she was a Visiting Scholar with the 5G Innovation Centre (5GIC), Institute of Communications (ICS), University of Surrey, U.K. Her current research interests include wireless communications, including new air interface design, receiver design, and iterative signal processing for wireless communication systems.

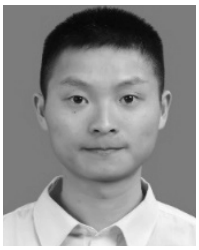

KAI MEI (S'17) received the bachelor's degree from the National University of Defense Technology, in 2017, where he is currently pursuing the Ph.D. degree. His research interests include synchronization and channel estimation in OFDM systems and MIMO-OFDM systems, and machine learning applications in wireless communications.

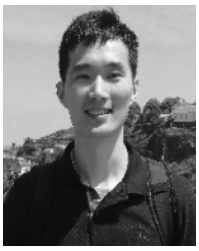

XIAORAN LIU received the B.S. and M.S. degrees from the National University of Defense Technology, Changsha, China, in 2014 and 2016, respectively, where he is currently pursuing the Ph.D. degree with the School of Electronic Science. His research interests include wireless communications technology, optimization method, and 5G technology.

LEI ZHANG received the B.Eng. degree in communication engineering and the M.Sc. degree in electromagnetic fields and microwave technology from Northwestern Polytechnic University, China, and the Ph.D. degree from The University of Sheffield, U.K. He was a Research Fellow with the 5G Innovation Centre (5GIC), Institute of Communications (ICS), University of Surrey, U.K. He is currently a Lecturer with the University of Glasgow. He holds more than ten international patents on wireless communications. His research interests include communications and array signal processing.

JIBO WEI received the B.S. and M.S. degrees in electronic engineering from the National University of Defense Technology (NUDT), Changsha, China, in 1989 and 1992, respectively, and the Ph.D. degree in electronic engineering from Southeast University, Nanjing, China, in 1998. His research interests include wireless network protocol and signal processing in communications, more specially, multicarrier transmission, cooperative communication, and cognitive networks.